Self-Consistency of Polarization Diversity Measurement of Rainfall

G. Scarchilli, E. Gorgucci, V. Chandrasekar, *Member, IEEE,* and A. Dobaie

Abstract— **Polarization diversity measurements of rainfall, namely the reflectivity factor, differential reflectivity, and specific differential propagation phase, vary in a constrained three-dimensional space. Algorithms are derived to quantify this self-consistency of measurements. In particular, estimation of the specific differential propagation phase shift based on reflectivity and differential reflectivity is analyzed in detail. Theoretical simulation as well as radar observations of rainfall at S (CSU-CHILL) and C (Polar 55C) bands are used to demonstrate that the range profiles of differential propagation shift can be constructed from measurements of reflectivity and differential reflectivity.**

I. Introduction

POLARIMETRIC radar observation of rainfall has reached considerable level of maturity that it is starting to move into the mainstream of radar meteorology [1], [2]. This is due to the extensive observation of rain medium over a decade using several polarimetric radars and surface and airborne *in situ* measuring devices [1]–[5]. Theoretical calculation and radar observations suggest that the polarimetric measurements of reflectivity factor at horizontal polarization (Z_H) differential reflectivity (Z_{DR}) and specific differential phase (K_{DP}) lie in a limited three-dimensional space for rain medium. In other words, there is self-consistency in polarization diversity radar measurements of rainfall. This self-consistency feature has been used in several applications. Aydin *et al.* [6] have used the deviation from the self-consistency region of (Z_H, Z_{DR}) space to derive a hail detection signal (H_{DR}). Rain region in (Z_H, K_{DP}) space is used by [7] to discriminate between rain and hail. The self-consistency principle has been used by [8] to calibrate polarization diversity weather radar systems. In this paper we present the utilization of self-consistency in a more quantitative sense in comparison with the prior work in the literature. In other words, among the triplet of measurements Z_H, Z_{DR}, K_{DP}, we obtain estimates of one of the parameters based on the other two. Subsequently the accuracy of such an estimation procedure is evaluated. Theoretically there is no difference as to which measurement is predicted from the other two; however, in practice, there is a considerable difference. First, Z_H and Z_{DR} are measurements made at each range resolution volume whereas K_{DP} is obtained as a range derivative of the differential phase measurement (ϕ_{DP}), which is available at each range resolution. This is the fundamental difference between the measurement pairs (Z_H, Z_{DR}) and K_{DP}. In this paper, we demonstrate using theoretical analysis and radar observations, the estimation of one polarimetric radar measurement from the other two among the set (Z_H, Z_{DR}, and K_{DP}). The analysis is done for both S-band and C-band frequencies.

Our paper is organized as follows. The estimates of the polarimetric radar parameters based on the other two among the set Z_H, Z_{DR}, and K_{DP} is derived in Section II. In Section III simulations are used to study the error structure of the estimates. Section IV shows the evaluation of the estimates developed in Section II based on data collected in rainfall using the Polar 55C (polarimetric radar operated by CNR, Italy) and by the S-band CSU-CHILL radar. Section V summarizes the key results of this paper.

II. Theoretical Developments

Cloud models and measurement of Raindrop Size Distribution (RSD) at the surface show that a gamma distribution model adequately describes many of natural variations in the RSD [9]

$$N(D) = N_0 D^{\mu} e^{-(3.67+\mu)(D/D_o)} \quad (\mathrm{m}^{-3}\,\mathrm{mm}^{-1}) \tag{1}$$

where $N(D)$ is the number of raindrops per unit volume per unit size interval (D to $D + \Delta D$) and (N_o, D_o, μ) are parameters of the gamma distribution. The shape of a raindrop can be described by an oblate spheroid with the axis ratio (b/a) of the drop approximated by the relation [10]

$$\frac{b}{a} = 1.03 - 0.062\,D_e \tag{2}$$

where D_e is the equivolumetric spherical diameter of a raindrop in millimeters; a and b are the semimajor and semiminor axis of the raindrop. The radar parameters of the rain medium namely ($Z_{H,V}$, Z_{DR}, K_{DP}) can be expressed in terms of the RSD as follows [11]:

$$Z_{H,V} = \frac{\lambda^4}{\pi^5 |K|^2} \int \sigma_{H,V}(D) N(D)\, dD \quad (\mathrm{mm}^6\mathrm{m}^{-3}) \tag{3}$$

where $Z_{H,V}$ and $\sigma_{H,V}$ represent the reflectivity factors and radar cross sections at horizontal and vertical polarizations, respectively, λ the wavelength, and $K = (\epsilon_r - 1)/(\epsilon_r + 2)$ where ϵ_r is the dielectric constant of water:

$$Z_{DR} = \frac{\int \sigma_H(D) N(D)\, dD}{\int \sigma_V(D) N(D)\, dD} \tag{4}$$

$$K_{DP} = \frac{180\lambda}{\pi} \mathrm{Re} \int [f_H(D) - f_V(D)] N(D)\, dD \quad (\mathrm{deg} \cdot \mathrm{km}^{-1}) \tag{5}$$

Manuscript received January 24, 1995; revised June 15, 1995. This work was supported by the EEC program on the Environment "Storm '93" (PL910060: EC-1991-94, IFA-CNR), the National Group for Defense from Hydrogeological Hazards (CNR, Italy), and by the NSF (ATM-9200761).

G. Scarchilli and E. Gorgucci are with the Istitutto di Fisica dell'Atmosfera (CNR), Rome, Italy.

V. Chandrasekar and A. Dobaie are with the Colorado State University, Fort Collins, CO 80521 USA.

Publisher Item Identifier S 0196-2892(96)00301-4.

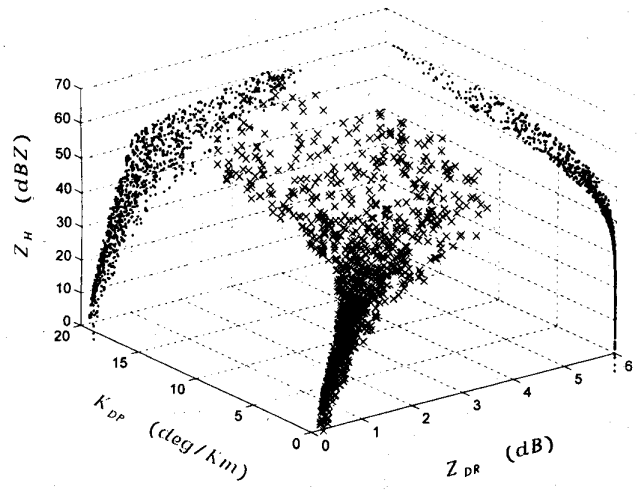

Fig. 1. Three-dimensional scatter diagram showing the relation between Z_H, Z_{DR}, and K_{DP} (x). The scatterplots on the walls show the conventional scatterplots between Z_H, Z_{DR} as well as Z_H, K_{DP}.

where f_H and f_V are the forward scatter amplitudes at H and V polarization, respectively. Rainfall rate and K_{DP} are nearly linearly related. Therefore, K_{DP} can be parameterized in a form similar to that of rainfall rate [12], [13] as

$$\hat{K}_{DP} = CZ_H^{\alpha}10^{-\beta Z_{DR}} \tag{6}$$

where Z_H is in units mm^6m^{-3} and Z_{DR} is in decibel. It should be noted that here $\hat{K}_{DP}$ indicates that the value of K_{DP} given by (6) is an estimate based on Z_H and Z_{DR} (and not from a profile of ϕ_{DP}).

The coefficients C and the exponents α and β are determined using a nonlinear regression analysis over a wide range of natural rainfall intensities as suggested by [9]. The parameters of the RSD (N_0, D_0, μ) can be varied to observe the variabilities in Z_H, Z_{DR}, and K_{DP}. Fig. 1 shows a three-dimensional scatter plot of Z_H, Z_{DR}, and K_{DP} obtained varying the RSD over a wide range of natural rainfall as suggested by [9]. The projections on each wall gives the commonly observed scatterplots of Z_H versus Z_{DR} and Z_H versus K_{DP}. The three-dimensional relations between Z_H, Z_{DR}, and K_{DP} are quantified in this paper. The values of the coefficients C, α and β in (6) at S and C bands are as follows:

S band (10 cm) $\quad C = 1.05\,10^{-4} \quad \alpha = 0.96 \quad \beta = 0.26$

C band (5.5 cm) $\quad C = 1.46\,10^{-4} \quad \alpha = 0.98 \quad \beta = 0.2.$

Fig. 2 shows the performance of the regression in (6) via scatter plot where $\hat{K}_{DP}$ is plotted against K_{DP}, for both S [Fig. 2(a)] and C bands [Fig. 2(b)]. The slope and correlation coefficient of the data are 1.0 and 0.9987 in Fig. 2(a) and 1.0 and 0.9989 in Fig. 2(b), respectively. It can be seen from Fig. 2 that the scatter is fairly small about the 45° line, thereby indicating that K_{DP} can be estimated reasonably well from Z_H and Z_{DR}. Equation (6) can be rearranged to express Z_H in terms of (Z_{DR}, K_{DP}) as well as Z_{DR} in terms of Z_H and K_{DP} as follows:

$$Z_H = \left(\frac{1}{C}\frac{K_{DP}}{10^{-\beta Z_{DR}}}\right)^{1/\alpha} \tag{7}$$

$$Z_{DR} = \frac{1}{\beta}\left(\log_{10} C + \log_{10} K_{DP} - \frac{\alpha}{10} dBZ_H\right) \tag{8}$$

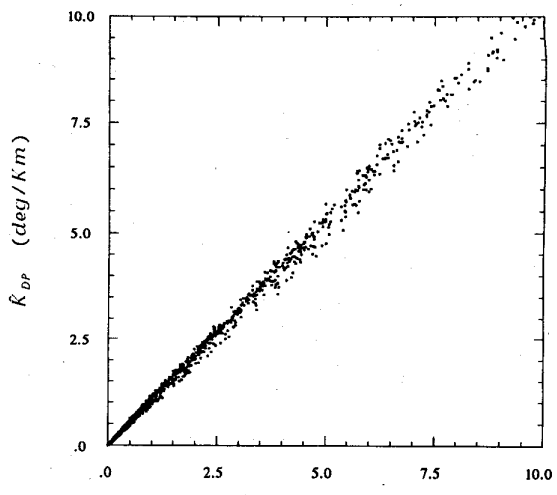

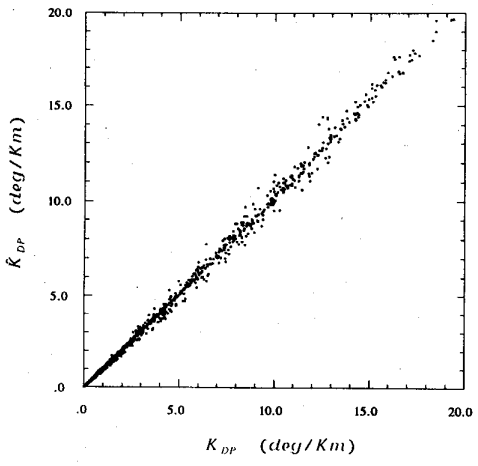

Fig. 2. (a) Scatter plot between the estimator of K_{DP} versus true K_{DP} at S-band. (b) Scatter plot between the estimator of K_{DP} versus true K_{DP} at C-band.

where $dBZ_H = 10\log_{10} Z_H$. However, (7) and (8) are not as robust as (6) in the presence of measurement errors.

III. Simulation and Error Studies

A. Error Analysis

The average standard errors in the estimate $\hat{K}_{DP}$ at S and C bands [Fig. 2(a) and (b)] are of the order of 10%. The scatter in Fig. 2 will increase in the presence of measurement fluctuations. The Fractional Standard Error due to measurement fluctuations can be obtained using error analysis procedures similar to those described in [13]:

$$FSE = \frac{\text{var}(\hat{K}_{DP})]^{0.5}}{\langle \hat{K}_{DP} \rangle} = [0.053\alpha^2 \text{var}(10\log Z_H) + 5.3\beta^2 \text{var}(Z_{DR})]^{0.5} \tag{9}$$

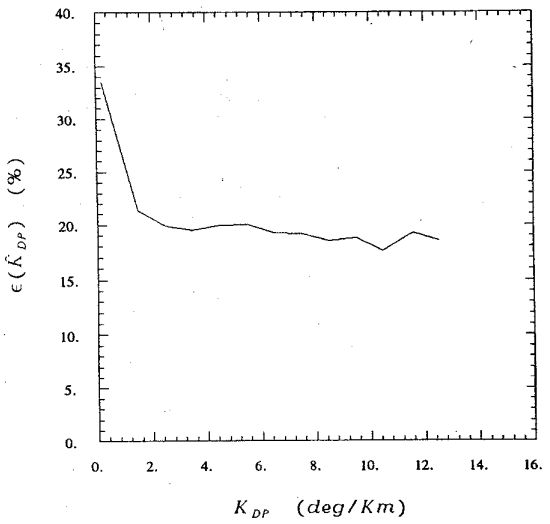

Fig. 3. Fractional standard error in the estimate $\hat{K}_{DP}$ as a function of K_{DP}.

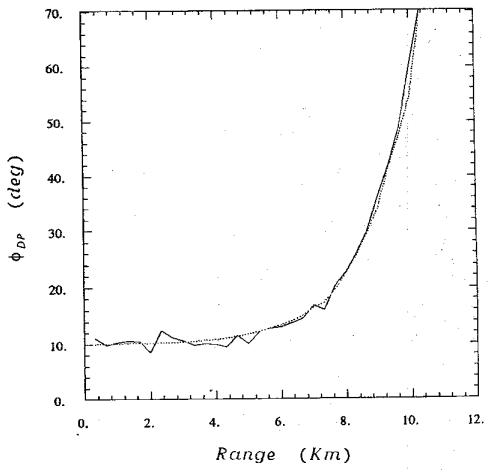

Fig. 4. Range profiles of reconstructed (dotted line) and true Φ_{DP} (solid line).

where var denotes the variance and $\langle\,\rangle$ denote the mean value. Z_H and Z_{DR} can be estimated to typical accuracies of 0.8 dB and 0.2 dB, respectively [14]. Under these conditions the fractional standard error of the estimate $\hat{K}_{DP}$ is approximately 20% at any value of Z_H and Z_{DR}. However, some range averaging of Z_H and Z_{DR} can make the estimate $\hat{K}_{DP}$ more accurate than 20%. The profile of ϕ_{DP} can be constructed as the integration of K_{DP} estimates over the range

$$\hat{\Phi}_{DP} = 2\int_0^R \hat{K}_{DP}(r)\,dr. \tag{10}$$

B. Simulation Study

In this section simulation techniques are used to evaluate the estimates derived in Section II. The simulation procedure used here is described in [15]. Single range gate samples as well as range profiles of multiparameter measurements are simulated. The single range gate samples are simulated to study the net error in the K_{DP} estimates based on measurement fluctuations as well as physical variability, whereas the range profiles of Z_H, Z_{DR}, and K_{DP} are simulated to compare the range profiles of ϕ_{DP}.

C. Single Range Sample

Several samples of Z_H, Z_{DR}, and K_{DP} triplets are simulated in the presence of measurement error [16]. The simulation parameters are: a) wavelength, $\lambda = 10$ cm; b) sampling time, $T_s = 1$ ms; c) number of sample pairs, $N = 128$; d) Gaussian Doppler velocity spectrum with width of $w = 2$ ms^{-1}; and e) zero lag cross correlation between H and V signals, $\rho_H V(0) = 0.99$. Subsequently, $\hat{K}_{DP}$ and true K_{DP} are compared to evaluate the net standard error. Fig. 3 shows a scatter plot of the fractional standard error ϵ of $\hat{K}_{DP}$ as a function of K_{DP}. We can see from Fig. 3 that ϵ is high ($\approx$35%) for very low values of K_{DP}; it decreases to approximately 20% for K_{DP} equal to 2 deg/km, which corresponds to the rainfall rate of about 40 mm/h and then FSE stays nearly constant with respect to rainfall rate. We note here that the 20% error rate includes the variabilities due to the physical process as well as the measurement errors.

D. Range Profile of Rain Path

We have simulated sample range profiles of Z_H, Z_{DR}, and K_{DP} with fairly moderate gradients in range to compare the true ϕ_{DP} with that estimated from Z_H and Z_{DR}. The model consists of a rain path where the reflectivity on dB scale is varied linearly along a path of 10 km with the reflectivity gradient equal to 3 dB/km and the range resolution of 50 m. To achieve this we have considered an exponential variation of the parameter N_o and fixed values of the parameters D_o and μ at each range gate. The measurement fluctuation is introduced at each range sample. Fig. 4 shows the profile "measured" and estimated ϕ_{DP} obtained using (10). Fairly good agreement can be seen between the "measured" profile of ϕ_{DP} and the estimated profile of ϕ_{DP} from Z_H and Z_{DR}. We have also evaluated the rain model where the reflectivity on dB scale varies as a triangle along the path of 10 km (not shown here) The error structure is similar to that of uniform path.

IV. Data Analysis

A. C-Band Data

Range profile data collected over rainfall regions by the Polar 55C (which is a C-band polarimetric radar operated near Florence, Italy) is used to demonstrate the self-consistency of the radar parameters. Details about the Polar 55C radar can be found in [17]. Data presented here was collected through a rainstorm that occurred near Florence, Italy, on November 16, 1992. The radar was operated in a time series mode, where the full time series was collected over a path of 10 km while the antenna was held stationary at an elevation of 2.3°. The time samples were obtained with a PRT of 0.85 ms and range resolution of 62.5 m. Reflectivity factor at horizontal polarization, Z_{DR}, and ϕ_{DP} were computed from the time series data. Fig. 5(a) and (b) show sample range profile of Z_H

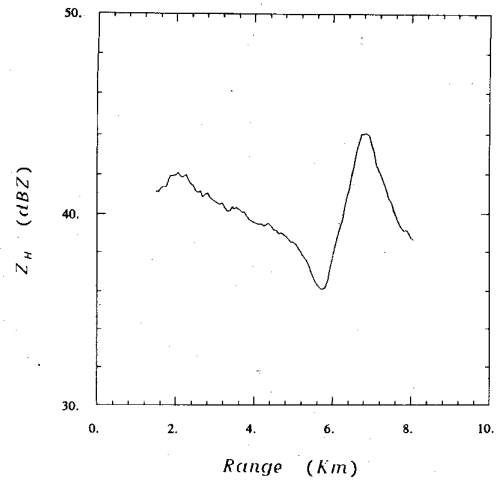

(a)

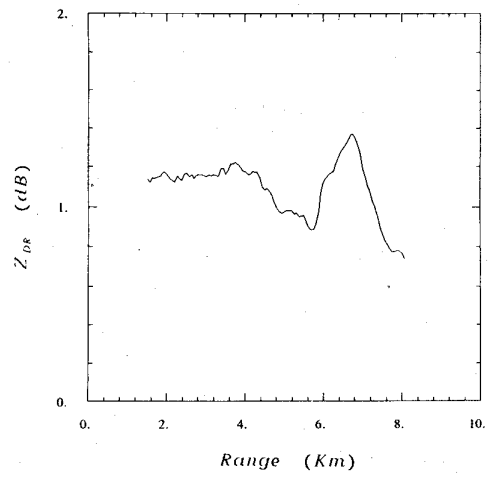

(b)

Fig. 5. (a) Range profile of reflectivity at horizontal polarization measured by Polar 55C. (b) Range profile of differential reflectivity measured by Polar 55C.

and Z_{DR} in the rainstorm. Fig. 6 shows the corresponding range profiles of Φ_{DP}, as well as $\hat{\Phi}_{DP}$ which is constructed from $\hat{K}_{DP}$. We note here that Φ_{DP} value at the initial range in the storm is not zero due to the radar system Φ_{DP} which is a fixed constant. We can see that the profiles of Φ_{DP} and $\hat{\Phi}_{DP}$ agree very well.

In the context of C-band radar data, a comment on the attenuation is appropriate at this point. It is well known that C-band radar signals experience attenuation and differential attenuation in moderate to heavy precipitation over long paths [15]. Attenuation and differential attenuation can be corrected in rainfall reasonably well using ϕ_{DP} [18]. The cumulative ϕ_{DP} along the rainpath gives an idea of attenuation suffered by C-band radar returns. The data shown in Figs. 5 and 6 have a total path integrated ϕ_{DP} of 10° approximately, implying the maximum cumulative attenuation in the data is not more than 0.5 dB. Therefore, we did not attempt to correct this data for attenuation. However, we recognize that for long

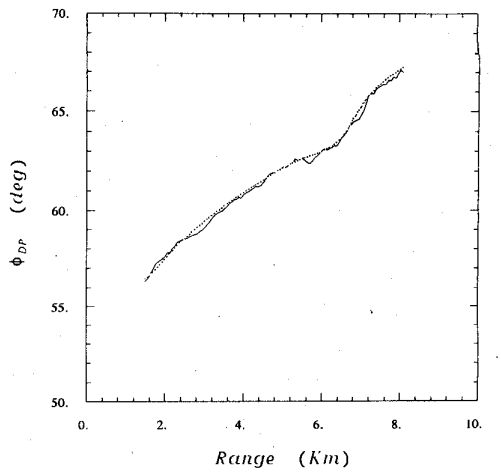

Fig. 6. Range profiles of $\hat{\Phi}_{DP}$ (dotted line) and Φ_{DP} (solid line) at C-band.

paths and intense storms (that may produce large values of cumulative ϕ_{DP}) we need to correct the Z_H and Z_{DR} profiles for attenuation before applying (6).

B. S-Band Data

The following shows data from the CSU-CHILL S-band polarization diversity radar system. The data shown here was collected on July 13, 1993, over an intense precipitation event in the vicinity of Denver, CO. The range profile was collected at an elevation of 1.8°. Fig. 7(a) shows a sample range profile of Z_H and Z_{DR} over the storm on July 13, 1993. The profile of Z_H with a 10 km swath exceeding 50 dBZ indicates that it is an intense precipitation event. Fig. 7(b) shows the profiles of Φ_{DP}, and $\hat{\Phi}_{DP}$ for the same data. It can be seen from Fig. 7(b) that the two profiles agree very well indicating self-consistency in the relation between Z_H, Z_{DR}, and ϕ_{DP}.

V. Conclusion

In this paper the self-consistency of the three common polarization diversity measurements in rainfall, namely reflectivity, differential reflectivity, and differential propagation phase shift, is studied. Based on the internal self-consistency of these measurements, the estimate of one of them is obtained based on the other two. Specifically the estimate of K_{DP} is analyzed in detail. K_{DP} is a range derivative of ϕ_{DP} which is directly measured at all range locations along with Z_H and Z_{DR}. Therefore, the estimates of K_{DP} based on Z_H and Z_{DR} are analyzed in detail.

It is shown that at both S and C band frequencies the variability between the estimated and true K_{DP} is fairly small and the fractional standard error in the estimate of $\hat{K}_{DP}$ is on average equal to 10% (in the absence of measurement errors). The FSE in the estimate of K_{DP} in the presence of measurement fluctuation was found to be about 20%. The above error estimates are based on single range measurements of Z_H and Z_{DR}. These errors can be reduced considerably with some range averaging. In addition the accuracy of the simulated differential phase ϕ_{DP}, which can be derived as the integration of K_{DP} estimates, was also verified. Finally

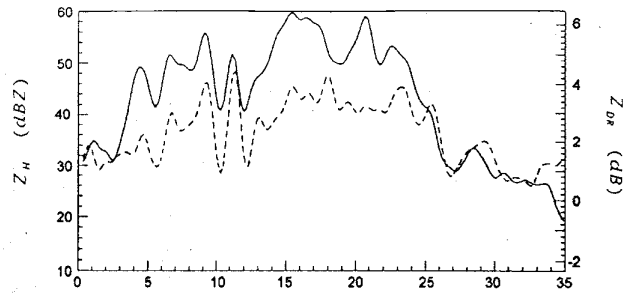

(a)

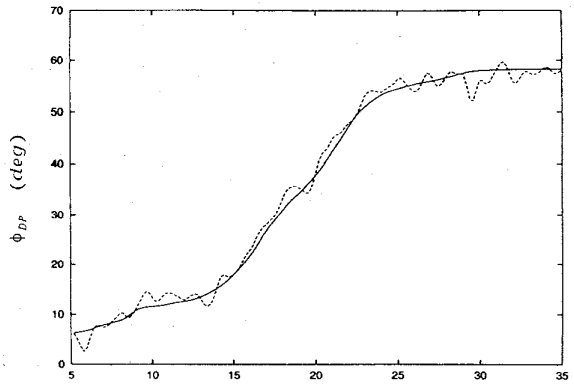

(b)

Fig. 7. (a) Range profiles of reflectivity at horizontal polarization Z_H (solid line), differential reflectivity Z_{DR} (dashed line) measured by CSU-CHILL radar. (b) Range profiles of $\tilde{\Phi}_{DP}$ (dotted line) and Φ_{DP} (solid line) at S-band.

the algorithms developed in this paper were tested using data collected in rainfall by a C-band (Polar 55C) and a S-band (CSU-CHILL) polarimetric radar. It is shown that the estimate of ϕ_{DP} based on range profiles of Z_H and Z_{DR} measurements works reasonably well. This self-consistency principle has potential application to detecting regions that have rain mixed with hail/graupel or detecting other contamination of the data such as ground clutter.

ACKNOWLEDGMENT

The authors acknowledge the valuable help of Prof. D. Giuli, Dr. L. Facheris, Dr. L. Baldini, and Dr. E. Palmisano for the cooperation regarding the radar data analysis. The authors would like to offer special thanks to G. Vezzani, A. Volpi, and P. Merendino of SMA who provided the technical support during the collection of radar data. The authors are grateful to P. Iacovelli for drafting and typing.

REFERENCES

[1] T. A. Seliga and V. N. Bringi, "Potential use of the radar reflectivity at orthogonal polarizations for measuring precipitation," *J. Appl. Meteor.*, vol. 15, pp. 69–76, 1976.

[2] R. J. Doviak and D. S. Zrnic, *Doppler Radar and Weather Observation*.San Diego, CA: Academic, 1993.

[3] T. A. Seliga, K. Aydin, and H. Direskeneli, "Disdrometer measurements during an intense rainfall event in central Illinois: Implications for differential reflectivity radar observation," *J. Climate Appl. Meteor.*, vol. 25, pp. 835–846, 1986.

[4] M. P. M. Hall, J. W. F. Goddard, and S. M. Cherry, "Identification of hydrometeors and other targets by dual-polarization radar," *Radio Sci.*, vol. 19, pp. 132–140, 1984.

[5] V. N. Bringi, R. M. Rasmussen, and J. Vivekanandan, "Multiparameter radar measurement in Colorado convective storms. Part I: Graupel melting studies," *J. Atmos. Sci.*, vol. 43, pp. 2545–2563, 1986.

[6] K. T. Aydin, A. Seliga, and V. Balaji, "Remote sensing of hail with a dual linear polarization radar," *J. Climate Appl. Meteor.*, vol. 25, pp. 1475–1484, 1986.

[7] N. Balakhrishnan and D. S. Zrnic, "Use of polarization to characterize precipitation and discriminate large hail," *J. Atmos. Sci.*, vol. 47, pp. 1525–1539, 1990.

[8] E. Gorgucci, G. Scarchilli, and V. Chandrasekar, "Calibration of radars using polarimetric techniques," *IEEE Trans. Geosci. Remote Sensing*, vol. 30, pp. 853–858, 1992.

[9] C. W. Ulbrich, "Natural variations in the analytical form of raindrop size distributions," *J. Climate Appl. Meteor.*, vol. 22, pp. 1764–1775, 1983.

[10] H. R. Pruppacher and R. L. Pitter, "A semi-empirical determination of the shape of cloud and raindrops," *J. Atmos. Sci.*, vol. 28, pp. 86–94, 1971.

[11] ——, "Differential reflectivity and differential phase shift: Application in radar meteorology," *Radio Sci.*, vol. 13, pp. 271–275, 1978.

[12] M. Sachidananda and D. S. Zrnic, "Rain rate estimates from differential polarization measurements," *J. Atmos. Oceanic Technol.*, vol. 4, pp. 588–598, 1987.

[13] E. Gorgucci, G. Scarchilli, and V. Chandrasekar, "A robust estimator of rainfall using differential reflectivity," *J. Atmos. Oceanic Technol.*, vol. 4, pp. 588–598, 1994.

[14] V. Chandrasekar and V. N. Bringi, "Error structure of multiparameter radar and surface measurement of rainfall: Part I," *J. Atmos. Oceanic Technol.*, vol. 5, pp. 783–795, 1988.

[15] G. Scarchilli, E. Gorgucci, V. Chandrasekar, and T. A. Seliga, "Rainfall estimation using polarimetric techniques at C-band frequencies," *J. Appl. Meteor.*, vol. 32, pp. 1150–1160, 1993.

[16] V. Chandrasekar, E. Gorgucci, and G. Scarchilli, "Optimization of multiparameter radar estimates of rainfall," *J. Appl. Meteor.*, vol. 32, pp. 1288–1293, 1993.

[17] G. Scarchilli, E. Gorgucci, D. Giuli, L. Facheris, and A. Freni, "Arno Project: Radar system and objectives," in *25th Conf. Radar Meteor.*, Paris, Amer. Meteor. Soc., 1991, pp. 805–808 (preprints).

[18] V. N. Bringi, V. Chandrasekar, N. Balakrishnan, and D. S. Zrnic, "An examination of propagation effects in rainfall on radar measurements at microwave frequencies," *J. Atmos. Oceanic Technol.*, vol. 8, pp. 829–840, 1990.

G. Scarchilli received the Italian degree in physics from the University "La Sapienza" of Rome, Italy.

In 1976, he joined the Institute of Atmospheric Physics (IFA) of National Research Council (CNR) as a Research Scientist. His research interests are radarmeteorology, signal processing, wave propagation, and scattering.

E. Gorgucci received the Italian degree in electronics engineering from the University "La Sapienza" of Rome, Italy.

He joined the Institute of Atmospheric Physics (IFA) of National Research Council (CNR) as a Research Scientist. His principal research fields are radarmeteorology, signal processing, and wave propagation.

V. Chandrasekar (S'84–M'87), photograph and biography not available at the time of publication.

A. Dobaie, photograph and biography not available at the time of publication.